Polyamide-6/silica nanocomposites

Garcia, M; Garcia-Turiel, J; Norder, B; Chavez, F; Kooi, BJ; van Zyl, WE; Verweij, H; Blank, DHA; Blank, Dave H.A.

Published in:
Advanced Engineering Materials

DOI:
10.1002/adem.200400059

Publication date:
2004

The thickness of the obtained structures in SU8-silver composite was measured by a surface profiler (Alpha-Step 500, TENCOR) and their electrical resistivity was characterized by resistivity meter four-point measurements (FPP-5000, VEECO). Impedance spectrometry was also employed in a four-point configuration to characterize the electrical behavior of the SU8-silver composite; Two LCR-meters were used alternatively to sweep a large frequency range, from 100 Hz to 10 MHz (HP4284A was used for the frequencies between 20 Hz and 1 MHz and HP 4285A for the frequencies between 75 kHz and 30 MHz).

[1] S. K. Bhattacharya, *Metal-filled polymers: properties and applications* (Eds: S. K. Bhattacharya), Marcel Dekker, INC., New-York **1986**.

[2] V. E. Gul', *Structure and properties of conducting polymer composites*, (Eds: V. E. Gul'), VSP BV, The Netherlands **1996**

[3] D. Lu, Q. K. Tong, *IEEE Transactions on electronics Packaging Manufacturing* **2000**, *22*, 228.

[4] M. Sun, *Microelectronics Journal* **2001**, *32*, 197.

[5] R. Strumpler, *J. Appl. Phys.* **1996**, *80*, 6091.

[6] H. Lorenz, M. Despont, *J. Micromech. Microeng.* **1997**, *7*, 121.

[7] M. O. Heuschkel, L. J. Guérin, *Sensors Actuators B* **1998**, *48*, 356.

[8] H. Lorenz, M. Despont, *Sensors Actuators A* **1998**, *64*, 33.

[9] S. Kirkpatrick, *Review of Modern Physics* **1973**, *45*, 574.

[10] R. Zallen, *The Physics of Amorphous Solids*, Vol. 11 (Eds: R. Zallen), Wiley, New- York **1983**.

[11] A. Y. Dovzhenko, P. V. Zhirkov, *Phys. Lett. A* **1995**, *204*, 247.

[12] I. Balberg,N. Binenbaum, *Phys. Rev. B* **1983**, *28*, 3799.

[13] F. Carmona, *Physica A* **1989**, *157*, 461.

[14] R. Biller, *J. Physics* **1985**, *18*, 989.

[15] G. R. Rushau, S. Yoshikawa, *J. Appl. Phys.* **1992**, *72*, 953.

[16] M. C. Peterman, P. Huie, *J. Micromech. Microeng.* **2003**, *13*, 380.

Polyamide-6/Silica Nanocomposites**

By *Monserrat García*,* *Javier García-Turiel*, *Ben Norder*, *Francisco Chavez*, *Bart J. Kooi*, *Werner E. van Zyl*, *Henk Verweij*, and *Dave H. A. Blank*

Growing research interest is focused on hybrid materials consisting of polymers containing nanoscale inorganic fillers,[1] because of the enhanced conductivity,[2,3] improved mechanical properties (e.g. stiffness and toughness),[4,5] and selective separation[6] that could result. Mechanical properties of filled polymers are mainly influenced and characterized by degree of dispersion, amount of filler added, crystallinity,

[*] *Dr. M. García, Prof. D. H. A. Blank*
Inorganic Materials Science and MESA+ Research Institute,
Faculty of Science and Technology
University of Twente,
P.O. Box 217, 7500 AE Enschede, The Netherlands
E-mail: m.m.garciacuriel@utwente.nl

J. García-Turiel
Van't Hoff Institute for Molecular Sciences
University of Amsterdam,
Nieuwe Achtergracht 166 ITS, 1018 WV Amsterdam, The Netherlands

B. Norder
Faculty of Applied Sciences
University of Technology,
Julianalaan 136, 2628 BL Delft, The Netherlands

Dr. F. Chávez
Department of Chemical Engineering
Princeton University,
NJ 08544, Princeton, USA.

Dr. B. Kooi:
Department of Applied Physics, Materials Science Group
University of Groningen
9747 AG Groningen, The Netherlands.

Dr. W. E. van Zyl
Department of Chemistry and Biochemistry
Rand Afrikaans University
P.O. Box 524, Auckland Park, 2006, South Africa

Prof. H. Verweij
Department of Materials Science and Engineering,
The Ohio State University
Columbus, OH 43210–1178, USA

[**] *The author thanks Prof. M.H. Wagner and Prof. O. Manero for their valuable feedback and Wim Vis and Tom Nijmeijer for the sample preparation. This work was performed with financial support from the Netherlands Organization for Scientific Research (NWO-PPM).*

  DOI: 10.1002/adem.200400059

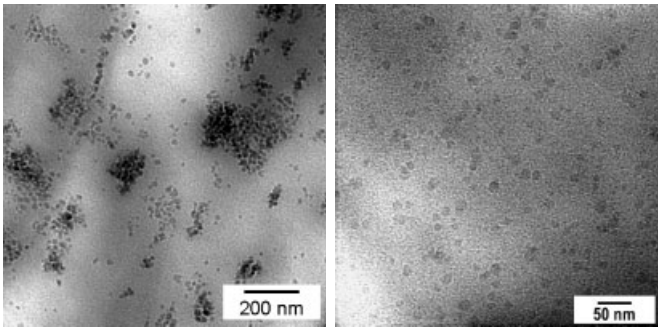

Fig. 1. TEM Picture of well dispersed silica 5 wt% (left) and 3 wt% (right).

apparent shear viscosity and dynamic mechanical experiments. Inhomogeneous filler distribution causes some regions to display close packed. A prominent physical effect of fillers in composites is the increase of the modulus. spheres (i.e. aggregates), whereas other parts of the composite material have lower volume fractions of spheres.[7] Specifically, the mechanical and physical properties of these types of materials are often dependent on the number, interspacing of the dispersed phase particles and particle size. As a matter of fact, it has been demonstrated that the physico-mechanical properties are better when the particle diameter is smaller.[8] This nanocomposites behavior has been attributed to the enhanced energy adsorptions as a result of the longer path which the crack has to go through because it has to pass by the numerous tiny particles, whereas the particle size play the role of stress concentrator.[9] Since heating is generally involved in plastic processing,[10] dynamic mechanical spectroscopy (DMS) and dynamic mechanical analysis (DMA) are powerful tools to follow changes in the modulus with increasing temperature. Analysis of rheological properties of filled polymers gives insight about the play of the inorganic particle in the pure polymer matrix. The flow behavior of polymer melts is of great importance in polymer manufacturing. Therefore, the description of flow phenomena by rheological studies is highly desirable to assist in the material (industrial) processability.[11,12] Polymer melt behavior is strongly affected by the presence of filler particles including its morphology, surface chemistry and concentration. Polyamides filled with silica nanoparticles have attracted interest

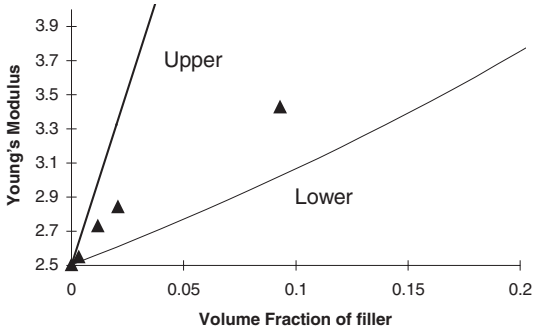

Fig. 2. Data for the PA-6 reinforced with silica particles indicating upper and lower bounds.

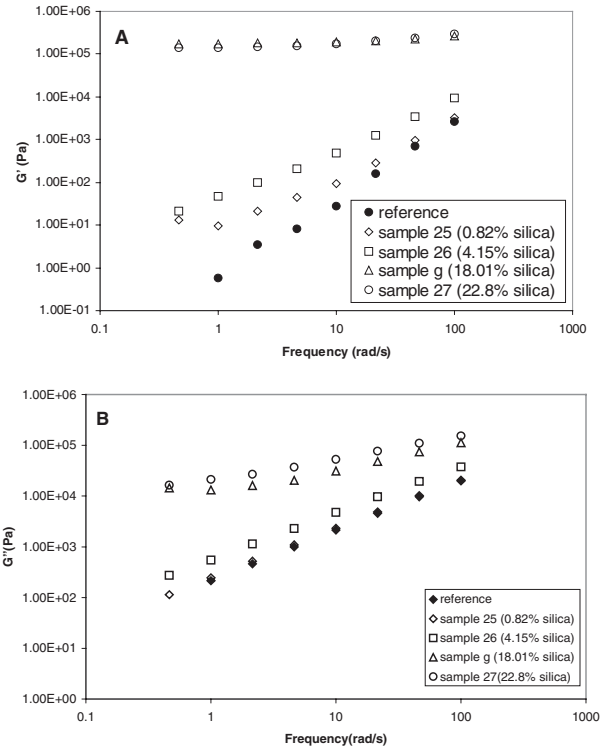

Fig. 3. Storage (A) and Loss (B) Modulus for PA-6 nanocomposites. The addition of silica particles changed drastically the viscoelastic properties of the unfilled polymer.

due to their effect on a variety of properties with small filler percentage (< 5 wt.-%) when compared to the neat polymer.[13,14]

In this study the influence of well-dispersed colloidal silica on the properties of the nanocomposites was analyzed. The mechanical properties (strain-stress curve) obtained from previous experiments were examined using the theorem of minimum potential energy in elasticity theory. Rheological experiments were performed on polymer melts with a wide range of silica loadings $\phi > 0.1$.

Results and discussion: A good dispersion was observed upon addition of 3 wt% and 5 wt% of silica sol as seen from the TEM picture of Figure 1.

Dry samples were used for the tensile tests to obtain E-modulus (see Tab. 3). Several models are available in the literature to account for the increase of elastic moduli with the presence of filler particles.[15–17] From the theorem of minimum potential energy in elasticity theory it is possible to obtain bounds for the elastic properties of a composite material.[18] A generalization of these bounds has been provided by Nielsen:[19]

$$C^n = \phi_f C_f^n + (1 - \phi_f) C_m^n$$

$$\eta_r = \eta_c / \eta_m \qquad (1)$$

where C stands for either the bulk modulus k, or the shear modulus, μ, the sub index f represents the filler properties, the sub index m the matrix properties, and ϕ_f represents the

Table 1. Slope of G′ and G″ of nanocomposites compared to PA-6.

Sample	wt%	Slope of G′	Slope of G″
Reference PA-6	0%	1.80	0.99
Sample 25	0.82%	1.09	0.97
Sample 26	4.15%	1.12	0.92
Sample g	18.01%	0.07	0.41
Sample 27	22.8%	0.13	0.42

volume fraction of the filler. Quantities without any sub index refer to the properties of the composite. Different values of the exponent n give rise to different forms of the law of mixtures. With n = –1, Eq. 1 is referred to as the series law of mixtures or the Reuss lower bound. With n = 1, Eq. 1 is referred to as the parallel law of mixtures or sometimes as the Voigt upper bound. Figure 2 shows a comparison of these bounds with the measured moduli for the composites considered in this work. Although these bounds provide theoretical limits for the values of the moduli, for typical composite materials they are too far apart (from the value here obtained) and are thus of limited practical value.

The role of the solid phase in the polymer matrix was obtained from the analysis of rheological properties. Two extremes set of value were analyzed. Samples with $\phi < 0.1$ and $\phi > 0.1$. The rheological behavior of PA-6 nanocomposites filled with silica nano-particles, is seen with the storage modulusG′(ω) and loss modulus G″(ω) plotted as a function of angular frequency (Fig. 3).

The storage modulus gives information about the elastic character of the fluid or the energy storage that takes place during the deformation. In Figure 3(a) is seen that curves for samples 25 (0.82 %silica) and 26(4.15 % silica) resulted with similar shape (similar elastic behavior) as the master curve for unfilled PA-6. The elastic behavior of samples with 0.82 % and 4.15 % silica does not differ much from that of the unfilled polymer. However, at low frequency range, an intermediate elastic plateau-like has been given an additional process of relaxation due to an adsorption of the polymer chain on the silica surface.[20] In both samples the storage modulus increases with the frequency. Nevertheless, curves from samples g (18.01 %) and 27 (22.8 %) show a different shape than those ones mentioned before. This substantial change in shape indicates a different elastic behavior due to the presence of silica. Both curves gave the same shape, therefore the elastic behavior of samples g and 27 might be similar. The behavior of G′ at low frequencies in the case of highly filled samples is likely due to network formation. The polymer chains are attached to the filler particles, and a continuous, physical network was formed.

The loss modulus gives the information about the viscous character of the fluid or the energy dissipation that occurs in flow. In Figure 3, the shape of the curves for samples 25(0.82 %silica) and 26 (4.15 % silica) are similar to the shape of the unfilled polymer, therefore similar viscous behavior is expected. Surprisingly, sample g and 27 differed substantially from the rest of the samples. That is also an indication that the viscous character of the samples g and 27 is different.

This effect is also observed in the slopes of the curves. The slopes are listed in Table 1. It is expected that at lower frequencies the polymer chains should be fully relaxed and exhibit characteristic homopolymer-like terminal flow behavior with slopes of 2 and 1 for G′ and G″. The slope of pure PA-6 is 1.80. This slope is in the range expected for polydisperse polymers.[21] Silica addition increases both the storage and loss modulus, but the effect in the slopes is greater for G′ than for G″. That is, the slope of the storage modulus decreases more pronouncedly when the amount of silica is higher in the sample than the slope of the loss modulus. Table 1.

If silica addition increases the storage modulus, it means more energy storage takes place during deformation and decreases the slope of the curve showing almost a plateau-like region. It is thought that the higher the G′and the smaller the slope, as it happens for samples g and 27, the more pronounced the interaction between the filler particles and network forming which implies that for these samples the viscosity is mainly caused by interactions between the particles and not by the viscosity of the polymer.

All these effects can be clearly seen by plotting the dynamic modulus G* and the phase angle δ as a function of angular frequency, see Figure 4.

Samples with silica percentage of 18.01 % and 22.8 % deviated from the results obtained by the other samples. The

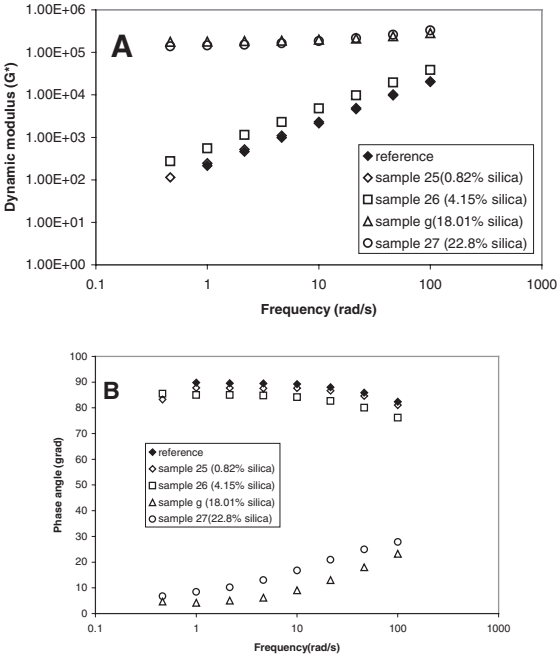

Fig. 4. Dynamic modulus(A) and Phase angle (B) for PA-6 nanocomposites.

ADVANCED ENGINEERING MATERIALS

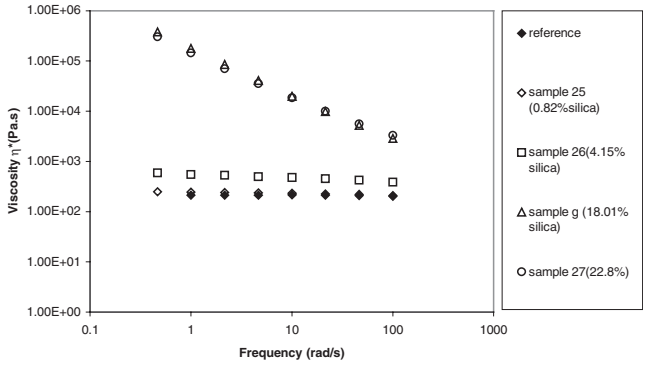

Fig. 5. Dynamic Viscosity (η^*) for PA-6 nanocomposites. The addition of silica particles shows a different effect at higher frequencies than that at lower frequencies.

highly filled polymer produced higher dynamic shear modulus. The same effect was already observed with PA6 and silica aerosil with ∅ ~ 640 nm.[22] Plots for dynamic modulus and phase angle showed identical shape at lower filler content and only above 20 % filler a clear deviation is observed. This indicates that only samples with 18.01 % silica and 22.8 % silica have a viscoelastic behavior that is significantly different from that of the reference. Therefore, the rheology of samples with higher filler content is dominated by particle-particle interactions. On the contrary, the phase angle of samples with 0.82 % and 4.15 % silica is not different from that of the unfilled polymer, indicating a rheological behavior dominated by the polymer matrix.

The slope of the dynamic modulus curves shows an interesting feature: at lower silica concentrations the slope of the loss modulus is very similar to the dynamic modulus, while at higher silica concentration the slope of the storage modulus is the one similar to the dynamic modulus. Increasing the silica content increases the amount of elasticity, at 18.01 % the rheological behavior is mainly elastic and G* shows a plateau at low frequencies.

Small strain shear viscosity: Figure 5 shows the dynamic viscosity plotted as a function of the frequency. Data is only given for small strain measurements. The shape of the curves for 0.82 % and 4.15 % silica is the same as the one of the unfilled polymer. Sample with 0.82 % showed almost no variation. In the sample with 4.15 % the viscosity was slightly increased (Newtonian behavior is observed).

Samples with high filler content showed a similar behavior between them, which differed substantially with the low filled samples. With the high-loaded samples the viscosity is likely dominated by the particle-particle interaction. In these samples a slope of –1 is approached at small frequencies (i.e. the shear stress approaches a constant), which is an indication of the existence of a yield stress in these materials.

Comparison between the relative viscosities at higher and lower frequency: The relative viscosity is given by $\eta_r = \eta_c/\eta_m$, where ηc is the viscosity of the composite at given strain and η_m is the viscosity of the polymer matrix, also at a give strain. The relative viscosities are showed in Table 2.

Correlation between the dynamic viscosity and the amount of silica added to the samples was investigated. The addition of silica increases the viscosity at lower and higher frequencies. Pronounced increase of viscosity was observed at low frequencies. From the frequency sweep, it can be seen that at lower strains the amount of filler changes the viscosity dramatically. It can be observed an increase of 3 decades in the viscosity. This effect may also come from the fact that all samples show some post-condensation, as it can also be seen in the increase of dynamic modulus.

If the dynamic viscosities of these PA-6/silica composites are compared, where the silica particles have ϕ < 30 nm with the results obtained for the same system[23] but using aerosil particles as fillers (40 – 50 nm) for small strain measurements some special features are found (see Tab. 3).

At lower filler content the viscosities for samples with silica are slightly higher than for samples with aerosil, but for both series of samples the values are in the same or quite comparable order of magnitude. But comparing samples with higher filler content, it is clearly seen that for silica with ϕ < 30 nm the viscosity are increased more. It can be through decreasing the particle size and at large volume fractions, particle-particle interactions become more important giving a considerable viscosity increase.

Therefore, the addition of silica to PA-6 increased the elasticity and also the viscosity. The high elasticity of the nanocomposites is a consequence of a network of touching particles. Other mechanisms[23,24] that may explain the increase in the polymer elasticity involve the formation of an electrical layer which can increase the interaction between particles and contribute to the elasticity, Brownian motion and spinning of the spherical particles. The analysis of different mechanisms goes beyond this study. It[Unterstrichen] can however be said that as the concentration increases, particles start to enter the neighborhood of surrounding particles. This disturbs the flow around the particles and consequently increases viscosity. At low concentrations, bi-particle interactions are most probable, while at high concentration more than two particles can interact simultaneously. If particle interactions occur, the viscosity can increase dramatically. The concentration at which strong viscosity effects become noticeable depends on the morphology of the dispersed phase and on morphological parameters.

Table 2. Relative viscosities for PA-6 nanocomposites at lower and higher frequency (strain).

Sample	Filler content	Relative Viscosity	
		ω=1rad/s	ω=100rad/s
Sample 25	0.82%	0.99	1.08
Sample 26	4.15%	1.83	2.43
Sample g	18.01%	13.62	791.27
Sample 27	22.8%	15.65	640.48

Table 3. Dynamic viscosities for PA-6/silica and PA-6/aerosil nanocomposites at lower and higher frequency (strain). The smaller the particle the higher the increment of viscosity.

Sample	Filler content	Dynamic Viscosity(Pa.s)	
		ω=1rad/s	ω=100rad/s
Sample 26	4.15%	548.15	384.674
Sample g	18.01%	179000	2857.24
Sample Aerosil I	5%	420	360
Sample Aerosil II	20%	10200	1030

Since nylon-6 readily absorbs moisture, it is useful to know the values of key properties for specimens prepared under standard wet conditions, that is, when the composites were exposed to ambient conditions. Therefore additional experiments of DMA on wet and dry samples of the pure polymer/silica nanocomposites are currently being performed. At $\phi \leq 1$ filler content the overall modules (E′ and E″) increased. Figure 6 shows the experimental plots of log E′ (modulus) versus temperature from –120 °C to 220 °C at a fixed frequency (1 Hz) for the neat matrix and the composites filled with ϕ = 0.1. The addition of silica nanoparticles increased the modulus of the materials above and below the Tg. The log E″ (loss modulus) was higher than neat PA-6 as well.

Conclusions: The E-modulus values obtained from stress-strain measurements on dry samples were compared to theoretical predictions using the theorem of minimum potential energy in elasticity theory to obtain bounds for the elastic properties of the composite material.

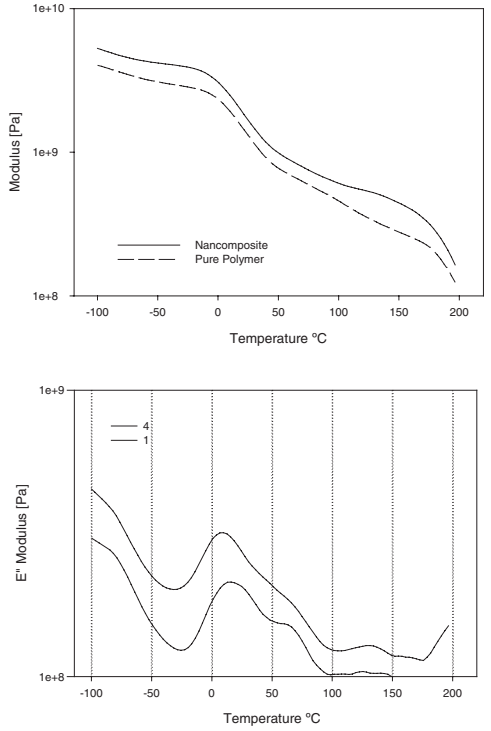

Fig. 6. Storage modulus (log E′) and loss modulus (log E″) versus temperature of pure PA-6 and nanocomposite with ϕ = 0.1.

Rheological measurements with two extreme sets of values were performed. The viscosity showed a very dependant behavior at different filler loadings. The viscosity of highly filled samples was mainly caused by interactions between particles and not by the viscosity of the polymer. Within the investigated shear rate domain, the composite behavior becomes all the more non-Newtonian as the filler loading increased. The deviation from the Newtonian behavior was attributed to the strong particle-particle interactions due to the extended surface areas, and hence to the tendency of silica particles to form aggregates. This was especially true in the case of the 18 wt% and 22 wt% silica loadings. Due to the fact that small strain viscosity increased upon the addition of the spherical particles, the mechanism most likely relies on the direct contact between particles. Large shear experiments would confirm this since the network formation would break down under large shear strain.

Experimental

Materials and Sample Preparation: Nylon-6 obtained from Sigma-Aldrich (The Netherlands) and silica sol SNOWTEX® (Nissan Chemical, Japan) were used. The preparation of the polymer-sol mixture has been described elsewhere.[25]

The dynamic mechanical spectra were recorded on a PerkinElmer DMA 7E Dynamic Mechanical Analyzer. Small rectangular bars of the samples, size approximately 1.25x3x20 mm, were subjected to a sinusoidal deformation at constant frequency, using a three point bending platform of 15 mm. Measurements were carried out at a fixed frequency of 1 Hz and a heating rate of 5 °C/min, in the temperature range between –100 °C and 200 °C. The amplitude of the sinusoidal deformation was 10 μm during the run. The static force was always 10 % more than the dynamic force, in order to ensure good contact between the probe and the sample. The data was collected using Pyris software for Windows, version 3.81.

Dynamic mechanical spectroscopy (DMS) was performed on the samples described above isothermally in a controlled-strain rate instrument ARES Rheometrics Spectrometer at a temperature of 230 °C. The angular displacement (or the angular velocity) is the independent variable and the viscous drag-torque the dependent variable. The linear viscoelastic strain limit of the composites was determined using strain sweeps experiments (where the –angular- frequency dependency of the polymer melt is determined). The dynamic viscosity and the shear modulus were both obtained by using a set of 25 mm diameter parallel plates, and frequency sweeps were from 10^{-2} to 10^{3} rads^{-1} (Hz) at a 100 % strain level. Measurements were performed from high to low frequencies after residence times of 5, 10 and 15 mins respectively under nitrogen atmosphere. Once the material was mounted on the rheometer the sample was compressed to a 2 mm plate gap.

Prior to the DMA measurements, the film-cast nanocomposites were compression molded into sheets of size 19 × 5.5 × 1 mm at 250–260 °C. Prior to testing, sample strips of 25 × 2–3 × 0.5–1 mm were made. For the tensile test, the samples were dried in a vacuum oven at 80 °C for 2 days. Plates of 1 mm thickness were molded and the test samples were machined out of the plates. The elastic modulus was measured at a tensile speed of 1 mm/min and the displacement was measured with an extensometer with a gauge length of 10 mm. Transmission Electron Microscopy (TEM) micrographs were obtained using a JEOL 2010F equipped with a field-emission gun operating at 200 kV. TEM samples were prepared by ultramicrotoming thin sections of the nanocomposites with a diamond knife. These thin sections were then captured on Formvar coated Ni grids. The particles observed in the micrographs were unambiguously identified as silica by using both X-Ray Energy Dispersive Spectrometry (EDAX R-TEM Sapphire detector equipped with a super-ultra thin window) and Energy Filtering (Gatan Imaging Filter 2001) attached to the TEM.

Received: November 20, 2003
Final version: June 14, 2004

[1] I. Honma, S. Nomura, H. Nakajima, *J. Membrane Sci.* **2001**, *185*, 83.
[2] E. Coronado, J.-R. Galan-Mascaros, C.-J. Gomez-Garcia, V. Laukhin, *Nature* **2000**, *408*, 447.
[3] F. Croce, G.-B. Appetecchi, L. Persi, B. Scrosati, *Nature* **1998**, *394*, 456.
[4] B. 6M. Novak, *Adv. Mater*. **1993**, *5*, 422.
[5] T. J. Pinnavaia, *Science* **1983**, *220*, 365.
[6] T. C. Merkel, B.-D. Freeman, R.-J. Spontak, Z. He, I. Pinnau, P. Meakin, A.-J. Hill, *Science* **2002**, *296*, 519.
[7] E. Reynaud, T. Jouen, C. Gauthier, G. Vigier, J. Varlet, *Polymer* **2001**, *42*, 8759.
[8] G. C. Richardson, J.-A. Sauer, *Polym. Eng. Sci.* **1976**, *16*, 252.
[9] N. S. Enikolopyan, M. L. Fridman, I. O. Stalnova, V. L. Popov, *Adv. Polym. Sci*. **1990**, *96*, 1.
[10] A. A. Berlin, S. A. Volfson, N. S. Enikolopyan, S. S. Negmatov, *Principles of Polymer Composites*, SPRINGER-VERLAG, **1986**, Ch. 1.
[11] D. W. Van Krevelen, Properties of Polymers. *Their estimation and correlation with chemical structure*. ELSEVIER, Amsterdam **1976**, 280.
[12] B. J. Holland J.-N Hay, *Polym. Int*. **2000**, *49*, 943.
[13] F. Yang, Y. Ou, Y. -Z. Yu, *J. Appl. Polym. Sci.* **1998**, *69*, 355.
[14] Y. Ou, F. Yang, Z. Yu, Z. *J. Polym. Sci.: Part B* **1998**, *36*, 789.
[15] E. H. Kerner, *Proc. Phys. Soc*. **1956**, *B69*, 808.
[16] Z. Hashin, *J. Mech. Phys. Sol*. **1991**, *39*, 745.
[17] T. Mori, K. Tanaka, *Acta Metall*. **1973**, *21*, 571.
[18] R. M. Christensen, *Mechanics of Composite Materials*, JOHN WILEY & SONS **1979**.
[19] L. E. Nielsen, R.-F. Landel, *Mechanical Properties of Polymers and Composites*, M. DEKKER, New York **1994**.
[20] Cassagnau, P. *Polymer* **2003**, *44*, 6607.
[21] A. Y.Malkin, *Adv. Polym. Sci*. **1990**, *96*, 69.
[22] G. Wu, S. Asai, M. Sumita, T. Hattori, R. Higuchi, J. Washiyama, *Coll. Polym. Sci*. 278, **2000**, 220.
[23] M. van Es, *Polymer-Clay Nanocomposite*s, Thesis University of Delft. The Netherlands. **2001**, 178.
[24] J. Mewis, C. W. Macosko, *Rheology Principles, Measurements, and applications*, WILEY-VCH, New York **1994**, Chap. 10.
[25] W. E. van Zyl, M. Garcia, B.-A. G. Schrauwen, B Kooi, J. Th. de Hosson, H. Verweij, *Macromol. Mater. Eng*. **2002**, *287*, 106.

Smart Nanostructured Polymeric Coatings for Use as Remote optical Strain Sensors**

By *Jérôme Halary*, *Paul Cookson*, *John L. Stanford*, *Peter A. Lovell*, and *Robert J. Young**

Smart materials can be defined as materials that incorporate the functions of sensing, actuation and control. In this study, we aimed to develop a novel high-resolution, non-contact Raman technique to measure surface stresses and strains of a wide range of Raman-inactive engineering components.

It is widely recognised that some crystalline materials are capable of undergoing stress/strain induced Raman band shifts.[1,2] As a material is strained, the interatomic distance changes, giving rise to a change in the interatomic force constant, and therefore a change in the vibrational frequency. Following the peak position enables the stress or strain applied to that material to be measured. A recent study in Japan,[3] has reported the development of PbO coatings for strain measurement applications. Such coatings, however, are brittle (breaking strain ~ 0.5 %) and have relatively small strain-induced Raman band shifts (~ –2 cm^{-1} / % strain) with substantial errors arising from the weak Raman scattering.

The present study is concerned with the development of stress-sensitive coatings by combining materials that undergo resonant Raman scattering within high performance polymer matrices. Polyurethanes were therefore used because of their excellent and wide-ranging physical properties and ease of processing. Two types of coatings were developed: (i) microphase-separated copolyurethanes (DA-coPU) where the Raman active species are nanoscale-dispersed diacetylene-containing hard segments (DA) that are produced *in situ* and (ii) polyurethane nanocomposites (SWNT-PU) filled with dispersed HiPco single-wall carbon nanotubes.

Polydiacetylenes[4,5] and DA-coPU systems have been extensively studied in the past fifteen years,[6–9] whereas most research based on embedded nanotubes is usually centred on epoxy resins or PMMA as matrices.[10–15]

[*] *J. Halary, Dr. P. Cookson, Prof. J. L. Stanford, Prof. P. A. Lovell, Prof. R. J. Young*
Manchester Materials Science Centre,
UMIST and The University of Manchester,
Manchester M1 7HS, UK
E-mail: jerome.halary@laposte.net

[**] *This work was supported by the Engineering and Physical Sciences Research Council (EPSRC) under the Grant GR/N27705/01*

 DOI: 10.1002/adem.200400061